Nanoscale

PAPER

View Article Online
View Journal | View Issue

Cite this: *Nanoscale*, 2015, **7**, 10259

Supramolecular fabrication of multilevel graphene-based gas sensors with high NO_2 sensibility†

Zhuo Chen,[a] Ahmad Umar,[b] Shiwei Wang,[a] Yao Wang,*[a] Tong Tian,[a] Ying Shang,[a] Yuzun Fan,[a] Qi Qi,[c] Dongmei Xu[c] and Lei Jiang[a,d]

Received 19th March 2015,
Accepted 1st May 2015

DOI: 10.1039/c5nr01770j

www.rsc.org/nanoscale

This study reports the supramolecular assembly of a silver nanoparticle-naphthalene-1-sulphonic acid-reduced graphene oxide composite (Ag-NA-rGO) and its utilization to fabricate a highly sensitive and selective gas sensor. The prepared supramolecular assembly acted not only as a non-covalent functionalization platform (π–π interaction) but was also an excellent scaffold to fabricate a highly sensitive and selective low concentration NO_2 gas sensor. The prepared composites were characterized using several techniques, which revealed that the graphene sheets were dispersed as ultrathin monolayers with a uniform distribution of silver nanoparticles. The fabricated multilevel structure exhibited an excellent sensing performance, *i.e.* 2.8 times better, towards 10 ppm NO_2 compared to the NA-rGO and rGO based sensors. Apart from its high sensitivity, superior reversibility and selectivity, the prepared supramolecular assembly exhibited an outstanding linear response over the large concentration range from 1 ppm to 10 ppm. The obtained results demonstrate that the prepared supramolecular assembly holds great potential in the fabrication of efficient and effective low-concentration NO_2 gas sensors for practical applications.

Introduction

Recently, graphene has attracted considerable attention due to its unique and outstanding characteristics such as high surface area, excellent electrical conductivity and mechanical flexibility, high thermal and chemical stability special structure and specific surface properties.[1–4] Since Geim and Novoselov[1] successfully exfoliated graphene from graphite, graphene, which is a single layer of carbon atoms with a honeycomb crystal lattice, has guided new directions not only in the areas of electronics, optoelectronics and energy but also in sensors and biological applications due to its unique two-dimensional sp^2-bonded structure.[2,3,5–8] The two most fascinating properties of graphene are its carrier-density dependent electrical conductivity and exceptionally high electron mobility.[9,10] The excellent properties of graphene are due to its unique band structure, which exhibits conduction and valence bands with near-linear dispersion that touch at the Brillouin zone corners to form a zero band-gap semiconductor.[11]

Because of its unique structure and unique properties, recently, graphene and graphene based composites have been considered as promising materials for gas sensing applications.[12–14] Therefore, functionalized graphene materials provide the perfect 2D platform with exceptional electronic properties for interactions between external molecules (gases and chemicals) and the functionalized groups on the modified graphene surface.[15] Thus, with such interactions, the electronic properties of materials change, which is the key factor to explain the sensing mechanisms of graphene-based sensors. For instance, the performances of graphene based gas sensors can be estimated by observing the variations in their electrical conductivity, which changes upon the adsorption of gaseous molecules on graphene surfaces. The adsorbed molecules change the local carrier concentration in graphene, which leads to step-like changes in resistance.[11] However, for practical gas sensing applications based on graphene or its composites, there are two important aspects that should be

[a]*Key Laboratory of Bio-Inspired Smart Interfacial Science and Technology of Ministry of Education, School of Chemistry and Environment, Beihang University, Beijing 100191, P R China. E-mail: yao@buaa.edu.cn*
[b]*Department of Chemistry, Faculty of Science and Arts and Promising Centre for Sensors and Electronic Devices, Najran University, Najran 11001, P.O. Box-1988, Kingdom of Saudi Arabia*
[c]*Gas and Humidity Sensing Department, Beijing Elite Tech Co., Beijing 100850, PR China*
[d]*Beijing National Laboratory for Molecular Sciences (MNLMS), Key Laboratory of Organic Solid, Institute of Chemistry, Chinese Academy of Sciences, Beijing 100190, China*
†Electronic supplementary information (ESI) available. See DOI: 10.1039/c5nr01770j

addressed, *i.e.* improving the dispersibility of graphene in solution[16,17] and enhancing its electronic properties in the solid state.[18]

To improve its dispersibility and sensibility, graphene oxide (GO) was chemically modified by functionalizing it *via* covalent bonding with certain functional groups, such as sulfophenyl, which has electron-withdrawing ability.[19] Although covalently bonded functionalized graphene-based materials can demonstrate good sensing performance, the original perfect atomic lattice of graphene is potentially sacrificed by the subsequently formed covalent bonds during the chemical modification process, which severely affects the intrinsic electrical properties of graphene. As a result, the electrical properties of graphene-based gas sensing materials are significantly decreased. Moreover, covalent chemical modification usually requires strict reaction conditions with complex chemical reaction processes and of course a relatively high cost, which restricts its widespread commercial application.[11]

Thus, to overcome such disadvantages of graphene, the strategy of supramolecular assembly based on non-covalent interactions, such as electrostatic forces, hydrogen bonding, π–π stacking, and hydrophobic interaction, is an alternative approach in which there is no covalent bonding effect at all on the intact structure of graphene due to the fact that only non-covalent interactions take place during the assembly.[20,21] In addition, supramolecular assembly offers more varieties of "guest substances" (*i.e.* inorganic ions, organic small molecules or macromolecules, and metallic nanoparticles) that can be assembled with graphene sheets.[22] Importantly, such supramolecular assembly can be prepared using facile processes at very mild temperatures. Thus, we believe that the fabrication of graphene-based gas sensors using supramolecular assembled materials is going to be a very promising research field. Furthermore, it provides the possibility of comprehensive integration of multifunction, which can stem either from the "guests" or graphene ("host") or both assembled composites.[23–27]

Based on the above mentioned idea, this study reports the fabrication of a highly sensitive, selective and reversible NO_2 gas sensor that is based on a multilevel silver nanoparticle (Ag)-naphthalene-1-sulphonic acid (NA)-reduced graphene oxide (r-GO) (Ag-NA-rGO) composite, which was prepared *via* supramolecular assembly. Here, naphthalene-1-sulphonic acid (NA), which has a large planar conjugated structure, was attached to r-GO through π–π stacking interactions and the silver nanoparticles were attached through electrostatic forces.

In the presented work, reduced graphene (rGO) was prepared as the one-level system (level I). Furthermore, sulfophenyl (Ph–SO_3^-), which has typical electron-withdrawing groups to NO_2, was introduced by supramolecular assembling of NA with GO through π–π stacking. After *in situ* reduction in hydrazine, the two-level (level II) assembly system, NA-rGO, was obtained, which was also used to study the NO_2 gas sensing characteristics. In order to further increase the system's adsorption capacity towards the sensing molecules,[28] silver nanoparticles were introduced in the system by electrostatic interactions as exceptional hydrophilic "guests". The prepared assembled multilayer was then *in situ* reduced to the three-level (level III) assembly system Ag-NA-rGO (Scheme 1).

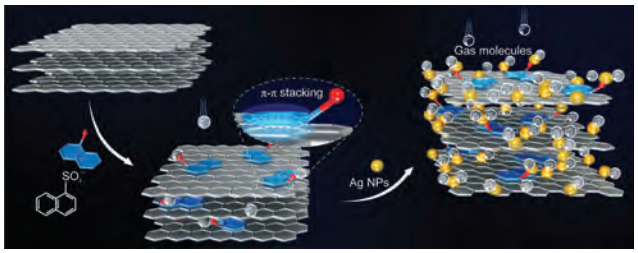

Scheme 1 Schematic illustration of the preparation of the Ag-NA-rGO supramolecular assembly for NO_2 gas sensing applications.

Thus, this work reports the fabrication and gas sensing performance of all three systems that were prepared, *i.e.* level I: rGO; level II: NA-rGO; and level III Ag-NA-rGO. Interestingly, it was observed that the NO_2 gas sensor that was fabricated based on the level III: Ag-NA-rGO system exhibited the highest gas sensing performance, and a maximum response to 10 ppm NO_2 can reach to 2.8 times and the sensing signal linearly increases even at low concentrations of NO_2 (1–10 ppm) in this system. Furthermore, the effect of the multilevel structure on the gas sensing performance was also systematically investigated in this work. To the best of our knowledge, this is the first ever report that demonstrates the NO_2 gas sensing performance of supramolecularly modified graphene. Thus, the presented work demonstrates a facile and effective approach for the fabrication of high-performance graphene-based materials for gas sensing applications.

Results and discussion

Fabrication of the graphene-based sensors

In the level I system, rGO was used as the basic gas sensing material, which can be readily prepared by the reduction of GO using hydrazine hydrate. GO has a regular C–C lattice, which can assemble with large conjugated molecules, such as benzene, naphthalene and anthracene, through π–π stacking to form supramolecularly modified graphene.[29,30]

For the level II system, the functional organic molecule, NA, with a large planar conjugated structure was selected owing to the fact that sulfophenyl is an electron-withdrawing group. The NA molecule is comprised of a naphthalene ring, which offers the intrinsic driving force for π–π stacking with graphene, and negatively charged terminals (–SO_3^-), which enhance hydrophilicity.[30,31] Thus, rGO was decorated *via* supramolecular modification, and hence NA-rGO was prepared after the reduction process.

In the level III system, silver (Ag) nanoparticles were introduced into the level II system *via* supramolecular assembly. The Ag nanoparticles were introduced in the system as another exceptional "guest" to further improve the gas sensing per-

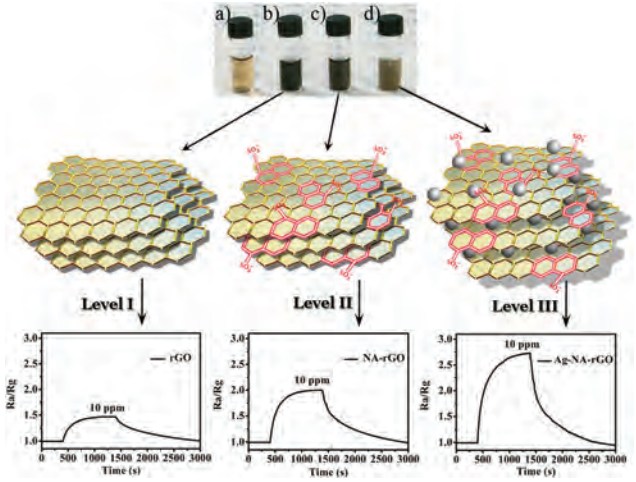

Fig. 1 Pictures of the (a) GO (b) rGO (c) NA-rGO and (d) Ag-NA-rGO solutions with the same concentration of 0.2 mg mL^{-1} and the ideal corresponding supramolecular assembly structures with different sensibilities of 1.3, 2.0 and 2.8 times greater towards 10 ppm NO_2.

formance of the prepared material. Precisely, the supramolecular driving force that was used to import the silver ions (Ag^+) was electrostatic interactions by which positive charged silver ions (Ag^+) were assembled with the sulfophenyl group (Ph–SO_3^-) on NA molecule and carboxylic groups (–COO^-) available on the GO surface. The major aim of incorporating Ag nanoparticles into the system was to isolate the graphene layers for enhancing the contact areas with the targeted gaseous molecules.

Importantly, it is worth mentioning that the water solubility of the NA-rGO and Ag-NA-rGO composites were greatly improved because of the hydrophilicity of the sulfophenyl groups in NA, which well resolved the puzzle of poor dispersibility of graphene. Fig. 1 exhibits the typical pictures of GO, rGO, NA-rGO and Ag-NA-rGO and their ideal supramolecular assembly structures with different sensitivities towards 10 ppm NO_2 gas for graphene-based sensors. The GO solution color was light brownish yellow (Fig. 1a); interestingly, the rGO solution color was darkened (Fig. 1b), which revealed that the graphene-oxide was successfully reduced; the formed NA-rGO solution also displayed a black color (Fig. 1c), while the Ag-NA-rGO solution possessed a dark green color (Fig. 1d). Importantly, all the prepared materials exhibited different sensibilities towards 10 ppm NO_2 gas (Fig. 1).

Characterizations of the graphene-based sensors

The ultrathin graphene sensing layer was deposited on the surface of a micro-grid array with a pure carbon film from its dispersion (0.2 mg mL^{-1}, same concentration as gas sensing test). Fig. 2a shows a typical transmission electron microscopic (TEM) image of a monolayer of Ag-NA-rGO. Silver nanoparticles were uniformly dispersed on the graphene sheet with similar scales, which ranged from 15 nm to 25 nm. Similar morphologies were also observed by atomic force microscopy

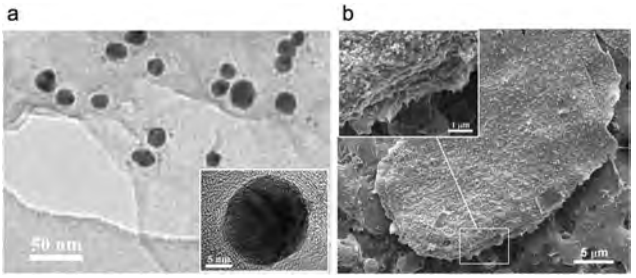

Fig. 2 (a) TEM image of a typical single layer of Ag-NA-rGO in different scales. (b) SEM image of typical multilevel Ag-NA-rGO sheet deposited on the surface of an interdigitated electrode.

(AFM), as shown in Fig. S1.† As evident from the AFM graph, the graphene sheets are well dispersed and they possess ultrathin monolayers. Furthermore, the silver nanoparticles are uniformly dispersed on the graphene sheet. According to the AFM measurement, the thicknesses of the Ag-NA-rGO sheets are approximately 1–1.5 nm.

Fig. 2b exhibits a typical scanning electron microscopy (SEM) image of a multilevel Ag-NA-rGO sheet coated on the surface of an interdigitated electrode (IE). The observed SEM image reflects the real morphology during the gas sensing test for using the same dispersion and devices. A multi-layer graphene sheet can be clearly seen together with uniformly distributed silver nanoparticles on the surface or among the layers. The multilevel structure is in conformity with the ideal supramolecular assembly structure, which was originally designed (Fig. 1d).

To examine their crystal quality and structures, the rGO, NA-rGO and Ag-NA-rGO hybrid composites were investigated using X-ray diffraction (XRD) and the results are shown in Fig. 3a. The XRD patterns for rGO and NA-rGO exhibit a single diffraction reflection at 22.78°, which is attributed to the diffraction from the (002) plane of the hexagonal graphite structure. The X-ray diffraction intensities of the rGO and NA-rGO composite reveal the degree of graphitization of the prepared materials. Interestingly, when the NA-rGO composite was modified with Ag nanoparticles, several new diffraction reflections are seen in the pattern, which are mostly related to the Ag ions. The Ag-NA-rGO composite exhibited several well-

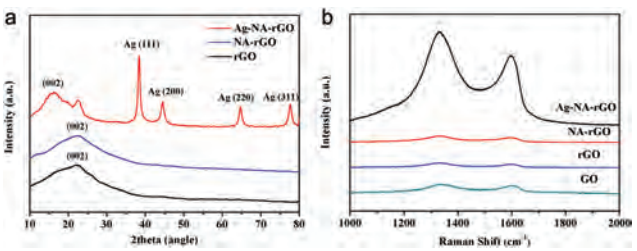

Fig. 3 (a) XRD patterns of rGO, NA-rGO and Ag-NA-rGO films and (b) Raman spectra of GO, rGO, NA-rGO and Ag-NA-rGO films.

defined diffraction reflections at 2θ = 38.34°, 44.52°, 64.68° and 77.58°, which are attributed to the (111), (200), (220) and (311) planes, respectively, and correspond to the face-centered cubic (fcc) structure of Ag nanoparticles[28,32] Interestingly, a new peak appeared at 16.12°, which indicates that the assembled Ag nanoparticles slightly increased the interlayer distance from 0.39 nm (2θ = 22.78°) to 0.55 nm (2θ = 16.12°).

Furthermore, the detailed structural properties of the prepared materials were examined by Raman scattering spectroscopy and the results are shown in Fig. 3b. The Ag-NA-rGO composite exhibits two very clear Raman bands that appear at 1329 cm^{-1} and 1597 cm^{-1}, which correspond to the D- and G-bands. It is well known that the intensity ratios of the D- and G-bands (I_D/I_G) are related to the structural defects, which are created by the functional groups on the carbon basal plane and disordered structures of the graphitic domains. Theoretically, a higher I_D/I_G value refers to fewer defects and possession of better structures. The I_D/I_G values for rGO, NA-rGO and Ag-NA-rGO were calculated and found to be 1.35, 1.34 and 1.35, respectively. These calculated values are higher than that of GO (1.15), which clearly exhibit the successful reduction of structural defects as most of the functional groups of GO were eliminated after reduction. Basically, similar to rGO, the I_D/I_G value of NA-rGO and Ag-NA-rGO is 1.34 and 1.35, respectively, which could be attributed to the special advantages of supramolecular modification for preserving the inherent structure of graphene rather than chemical modification. The intact structure with fewer defects would directly contribute to the promotion of conductivity, which plays a key role in gas sensitivity. Table S1† summarizes the Raman shift, peak intensities and intensity ratios (I_D/I_G) of all four samples, *i.e.* Ag-NA-rGO, NA-rGO, rGO and GO.

To investigate their surface properties, the prepared rGO, NA-rGO and Ag-NA-rGO were further characterized using X-ray photoelectron spectroscopy (XPS). As shown in Fig. 4, the XPS spectra exhibit the existence of elemental Ag and the elemental status of Ag (3d). The Ag (3d) peaks are a doublet, which arise from spin–orbit coupling ($3d_{5/2}$ and $3d_{3/2}$).[33] The binding energies of the Ag $3d_{5/2}$ and Ag $3d_{3/2}$ peaks are observed at 368.9 and 375 eV, respectively. The orbital interaction splitting of the 3d doublet of Ag was 6.0 eV and the typical binding energy values of bulk Ag were observed (the standard binding energy of Ag $3d_{5/2}$ for bulk Ag is about 368.2 eV), which suggest the formation of metallic silver. In addition, the asymmetric shape of the peaks also indicates the presence of metallic silver rather than silver oxide.[34] Moreover, we can further confirm that metallic silver exists in the Ag-NA-rGO composites through the XRD analysis. In addition, it can be proven from the observed spectrum that NA is complexed with graphene by supramolecular modification. Furthermore, quantitative analysis indicates that the proportion of carbon in the three sensing materials is 66.2%, 44.1% and 17.2%, which shows the successive decrease of carbon because of the addition of new elements in NA molecules and Ag nanoparticles.

The elemental composition of the prepared Ag-NA-rGO composite was further analyzed by energy dispersive spectroscopy (EDS) attached with TEM. Fig. S2† shows the typical EDS spectrum of the prepared Ag-NA-rGO composite, which exhibited several well-defined peaks that are related to C, O, S and Ag. It is clear from the observed EDS spectrum that the majority of content in the prepared composite is carbon with the total percentage of 56.3%. The Ag content in the composite is 22.5%, which proves that Ag is available in the prepared composite. Furthermore, the observed sulfur content in the prepared composite is 2.10%, which indicates the successful introduction of sulfophenyl groups *via* supramolecular interaction between NA and GO sheets.

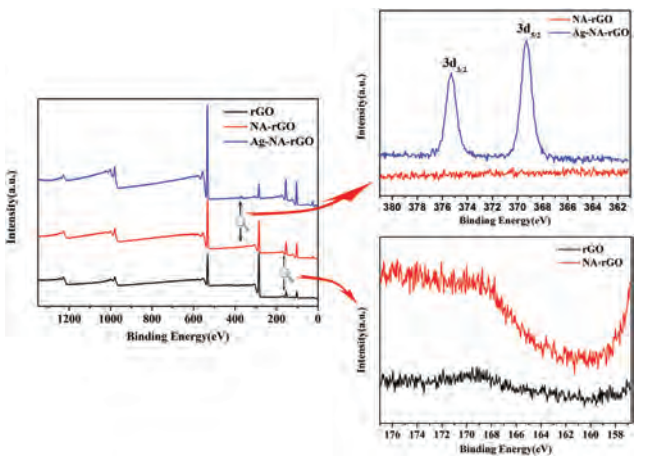

Fig. 4 Typical XPS of the prepared Ag-NA-rGO, NA-rGO and rGO materials.

Sensibility of the graphene-based gas sensors

The sensitivity of multilevel graphene-based sensors is based on the sensing materials that are used, and hence successive enhancements in the sensing responses were observed by the fabricated rGO, NA-rGO and Ag-NA-rGO based sensors. Chart S1† exhibits the ideal flow chart of gas sensing tests.

Fig. 5 illustrates the typical gas sensing responses of the rGO, NA-rGO and Ag-NA-rGO based sensors towards 10 ppm NO_2. Interestingly, the observed sensitivities for the fabricated gas sensors based on rGO, NA-rGO and Ag-NA-rGO hybrid composites were about 1.4, 2.0 and 2.8 times better, respectively.

The sensitivities of the fabricated sensors are evaluated by the ratio of the initial and final resistance (R_a/R_g), which were recorded under air and in the presence of NO_2 gas, respectively. This can be expressed by the following equation:

$$S = \frac{R_{air}}{R_{gas}} = \frac{\dfrac{R_0}{-q \times \sum \iint_{xy} \left(p_{air} \times \mu_p \times \frac{d\zeta}{d\chi} + D_p \frac{dp}{d\chi}\right) dxdy} + R_c}{\dfrac{R_0}{-q \times \sum \iint_{xy} \left(p_{gas} \times \mu_p \times \frac{d\zeta}{d\chi} + D_p \frac{dp}{d\chi}\right) dxdy} + R_c}$$

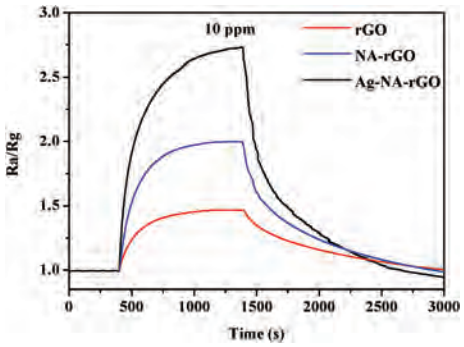

Fig. 5 Typical gas sensing responses of rGO, NA-rGO and Ag-NA-rGO hybrid composites based sensors towards 10 ppm NO_2 gas.

as $p = \frac{{n_i}^2}{n} = n_i \exp\left(\frac{E_i - E_F}{KT}\right)$ where R_0 is a constant, q is the quantity of electric charge, p_{air} and p_{gas} are the concentration of hole in air and NO_2 gas, respectively, $\sum \iint_{xy}$ is the total effective area, μ_p is the mobility of hole, ζ is the electric field intensity, D_p is the diffusion coefficient of hole, χ is the distance, R_c is the resistance from the films without sensing reaction, n_i is a constant, n is the concentration of electrons, E_i and E_F are the energy of the Fermi and the current material, K is the Boltzmann's constant, and T is the temperature.

Hole conductivity occurs along with percolation paths *via* grain-to-grain contacts and therefore depends on the value of the Schottky barrier of the adjacent grains.[35,36] For the level I system, rGO with a typical p-type semiconductor with holes as its main carriers was used (Fig. 6, level I). However, when the r-GO was functionalized with NA, the concentration of holes (P_{gas}) of NA-rGO enhanced because of the electronic absorption capacity of the sulfophenyl groups in NA (Fig. 6, Step 1, level II). In addition, the oxidized gas (NO_2) tends to absorb the lone pair electrons on electron-rich sites such as S or O atoms in SO_3^-, and thus NA-rGO would be further hole-doped (P_{gas}) because of the improvement of the electron-withdrawing ability of the sulfophenyl groups after NO_2 adsorption. Thus, the sensitivity of level II was enhanced significantly.

For Step 2, in the level III system in which the Ag-NA-rGO hybrid composite was used (Fig. 6, level III)), the silver nanoparticles play a very important role in isolating the graphene layers. The Ag nanoparticles segregate the graphene layers from a holistic entity into a multi-layer structure, hence permitting the penetration of NO_2 and the reaction with interlayers, followed by the reduction in the resistance without sensing reactions (R_c). Moreover, the isolation of layers can also cause the decrease of χ, namely, the increase of the change rate of electric field $\left(\frac{d\zeta}{d\chi}\right)$, together with the increase of total effective area $\sum \iint_{xy}$. In addition, the gas adsorption ability of the silver nanoparticles contributed the sensor to absorb extra NO_2 molecules, which resulted in the enhancement of the doping level (P_{gas}). Therefore, the sensitivity of the fabricated gas sensor that was based on the level III system was further enhanced.

Apart from their superior response abilities, the fabricated sensors also showed good reversibility upon removing the adsorbed NO_2 molecules by switching to air (Fig. 6). The results can be attributed to the weak combination between NO_2 molecules and lone-pair electrons in the functional groups. Furthermore, the isolation of graphene layers by the silver nanoparticles led to the desorption of NO_2 molecules more easily.

Based on the above discussion, it is clear that the level III system, *i.e.* the Ag-NA-rGO hybrid composite, exhibited best sensing performance. Thus, to investigate its detailed sensing behavior and performance, the Ag-NA-rGO hybrid composite based sensor was examined under different concentrations of NO_2 gas and the observed results are shown in Fig. 7a.

Interestingly, it was observed that with increasing the concentrations of NO_2 gas concentration, from 1 ppm to 10 ppm, the R_a/R_g values increased significantly, which revealed that the fabricated gas sensor is highly responsive toward both low and high concentrations of NO_2 gas and approximately 1.3 times of resistance change was observed after exposure to 1 ppm NO_2. Furthermore, the detection limit of the fabricated Ag-NA-rGO hybrid composite based sensor was determined to

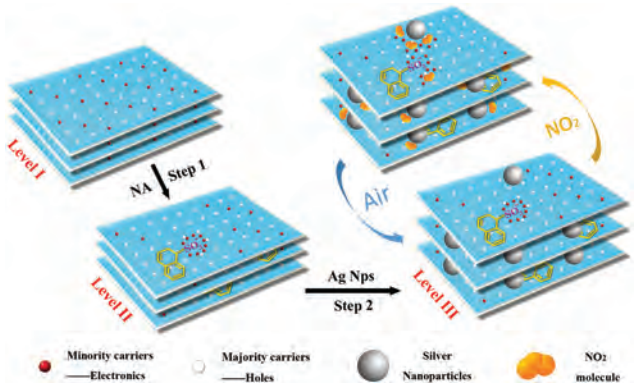

Fig. 6 The ideal gas sensing mechanism for the gas sensors fabricated based on multilevel hybrid composites.

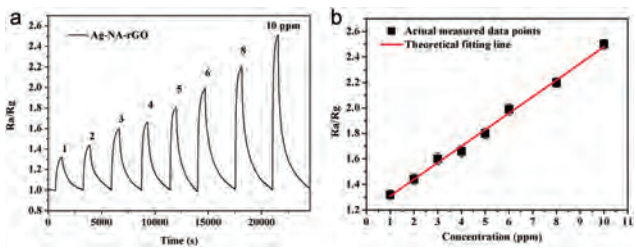

Fig. 7 (a) The responses of the Ag-NA-rGO based sensor towards various concentrations of NO_2 gas (from 1 ppm to 10 ppm), and (b) the linear relationship with NO_2 concentration in the range of 1 to 10 ppm. The error bars for each measurement lie within the symbols themselves.

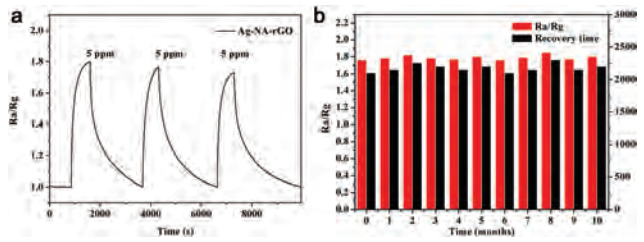

Fig. 8 (a) Reproducibility of the Ag-NA-rGO hybrid composite based sensor exposed to 5 ppm NO_2 gas for three successive response cycles. (b) Stability of the fabricated Ag-NA-rGO based sensor after exposing it in air for 10 months.

be 1 ppm. The fabricated Ag-NA-rGO based sensor showed an outstanding linear detection range towards NO_2 with different concentrations from 1 ppm to 10 ppm and the sensitivity was measured from 1.3 to 2.5 (Fig. 7b). The observed results clearly demonstrate an important and facile approach to detect the low concentrations of NO_2 for practical applications, and thus the presented approach to fabricate NO_2 gas sensors can be applied for practical device applications.

To verify the reliable reproducibility and high stability of the fabricated sensing devices, the Ag-NA-rGO hybrid composite based sensor was exposed to 5 ppm NO_2 for three successive cycles and results are shown in Fig. 8a. As evident from the observed results, the fabricated sensor exhibited a stable response with an average sensitivity of 1.76. Moreover, the response time and recovery time of the Ag-NA-rGO based sensor are 10 min and 40 min, respectively (Fig. 8a). It is also important to mention that the sensitivity of the fabricated Ag-NA-rGO based sensor floats slightly within 5.6% of its initial value after a 10-month aging process, as demonstrated in Fig. 8b. The observed results revealed that the fabricated Ag-NA-rGO hybrid composite based sensor exhibited very high stability, which is one of the key factors in commercialized gas sensors.

Selectivity is one of the most important characteristics of an efficient sensor; hence selectivity experiments were also performed for the fabricated Ag-NA-rGO based sensor. Several interfering gases such as acetone, ethanol, and ammonia (NH_3) were used for the selectivity experiments. Fig. 9 exhibits

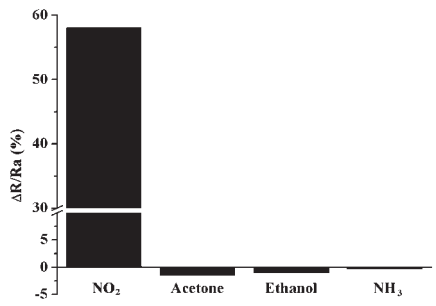

Fig. 9 Selective responses of the fabricated Ag-NA-rGO based sensor towards 10 ppm NO_2, acetone, ethanol and NH_3.

the typical gas responses for the Ag-NA-rGO based sensor towards 10 ppm NO_2, acetone, ethanol and NH_3. From the observed selectivity results, interestingly, it was found that the fabricated Ag-NA-rGO based sensor exhibited excellent selectivity towards NO_2 gas compared to the other gases such as acetone, ethanol and NH_3 that were used. It was amazing to see that the sensing response towards 10 ppm acetone was only −1.44, whereas the selective response of NO_2 can reach over 40 times of acetone. The observed results confirmed that the fabricated sensor is highly selective towards NO_2 gas.

Experimental section

The synthetic procedures for rGO, NA-rGO and Ag-NA-rGO were designed according to the reported literature.[16,37,38]

Preparation of graphene oxide (GO)

GO was purchased from XianFeng NANO Co., Ltd. To disperse the GO into water, in a typical process, 100 mg of GO was put in 100 mL de-ionized (DI) water under vigorous ultrasonication for 30 min. After ultrasonication, a good suspension of GO can be obtained.

Preparation of reduced graphene oxide (rGO)

To prepare rGO, in a typical reaction process, 4 mL of GO dispersion, 16 mL of deionized water, 75 μL of ammonia (30%) and 10 mL of hydrazine hydrate (1.12 μL mL^{-1}) were mixed under sonication in a 50 mL round bottom flask. Consequently, the obtained mixture was then heated at 95 °C in an oil bath for 1 h to obtain a stable rGO suspension.

Preparation of naphthalene-1-sulphonic acid sodium (NA) modified rGO (NA-rGO)

For the preparation of NA-rGO, typically 4 mL of GO dispersion was added in 10 mL of DI water to form a brown dispersion, followed by the addition of 92 mg of NA (Purchased from Alfa Aesar). Then, 5 mL of NaOH solution (4 mg mL^{-1}) was added dropwise to the dispersion, and the mixture was kept at 80 °C for 1 h under stirring after the addition of 10 mL hydrazine hydrate. The reduced GO product was rinsed with water several times and then re-dispersed in 20 mL of water under mild sonication.

Preparation of Ag-NA-rGO composites

To prepare the Ag-NA-rGO composite, 4 mL of GO dispersion was mixed with 10 mL of DI water in a 50 mL round bottom flask under stirring until a uniform brown dispersion was formed. Consequently, 92 mg of NA and 16 mg of silver nitrate were added in the resultant solution. After the addition of 5 mL of NaOH solution (4 mg mL^{-1}) and 10 mL hydrazine hydrate, the mixture was further stirred for 1 h at 80 °C in an oil bath. Finally, the obtained mixture was rinsed with water several times and the Ag-NA-rGO suspension was obtained after the product was re-dispersed in 20 mL of water by mild sonication.

Fabrication of gas sensors based on rGO, NA-rGO and Ag-NA-rGO composites

To fabricate the gas sensors, interdigitated electrodes (IE) were used, which were made of alumina ceramic chips with platinum microelectrodes fixed in them (each electrode has 10 pairs of digits). All the sensors were fabricated through the drop and dry method. In a typical fabrication process, 0.1 mL of rGO/NA-rGO/Ag-NA-rGO dispersion (0.2 mg mL^{-1}) was dropped on the surface of the IEs (10 pairs of digits with 5 μm fingers and 15 μm gaps, Synkera) and the coated IEs were dried on a heating plate in air at 50 °C for 10 min. After the drying process, a thin layer of rGO, NA-rGO, and/or Ag-NA-rGO was formed on the IEs, which were then connected by Alligator clips for sensing tests.

Sensing tests

All sensing tests were performed using a gas sensing system (CGS-1TP Intelligent Gas Sensing Analysis System, ELITE TECH. Chart S1†). For all the gas sensing measurements, a simple two-electrode configuration was employed. The sensitivities of the sensors were evaluated by measuring changes in the resistances, which were monitored by an automatic system. Prior to all gas sensing measurements, the gas cylinder was purged with pure air gas and after achieving a constant resistance, the fabricated sensors were sequentially exposed to NO_2 and air at room temperature (25 °C) in the range of 40%–70% relative humidity (RH). To check the reproducibility, all sensors were fabricated at least 3 times and characterized in terms of their sensing performances, and finally the average values were reported.

Characterizations of the rGO, NA-rGO and Ag-NA-rGO composites

The prepared sensing materials were characterized by several techniques. The surface morphology of the prepared Ag-NA-rGO composite was examined by atomic force microscopy (AFM; Dimension Icon instrument (USA)). The detailed structural properties of the prepared materials were examined by Raman-scattering spectroscopy (HORIBA Jobin Yvon Raman microscope (LabRAM HR800)) measured with a 514 nm laser at a power density of 4.7 mW. Surface properties were examined using X-ray photoelectron spectroscopy (XPS; ESCALAB 250 photoelectron spectrometer (ThermoFisher Scientific, USA)). The general morphologies of the prepared materials were examined by SEM (Quanta 250 FEG, FEI) and TEM microscopes (Sirion-200, Japan). All conductivity measurements were done by the conventional four-probe technique.

Conclusions

In summary, a multilevel supramolecular structure that is composed of NA and silver nanoparticles on rGO (Ag-NA-rGO) was prepared and used for the fabrication of a highly sensitive and selective NO_2 gas sensor. Interestingly, with the supramolecular modification, the water-solubility of the Ag-NA-rGO was greatly improved because of the hydrophilicity of the sulfophenyl groups in NA. In addition, the fabricated sensors tend to be hole-doped due to the electron withdrawing ability of NA, which results in the improvement of the sensitivities of the fabricated sensors. In addition, by introducing silver nanoparticles in the Ag-NA-rGO composite, the inherent ability to capture gaseous molecules and specific surface area was increased. The silver nanoparticles play a key role in the isolation of graphene layers and segregate the graphene layers from a holistic entity to a multi-layer structure, which permits the penetration of NO_2, and the reaction with interlayers causes significant improvement in the sensitivities of the fabricated Ag-NA-rGO based sensor. Moreover, the isolation of layers by silver nanoparticles provides enough space for gas desorption, which is beneficial to its reversibility. Compared with conventional graphene-based sensors, the multilevel Ag-NA-rGO-based sensors exhibited over 2.8 times greater response towards 10 ppm NO_2 and the sensing signals increases linearly in the concentration range from 1 ppm to 10 ppm. The presented work demonstrates a possibility to fabricate highly sensitive, reproducible, stable and selective gas sensors based on supramolecularly modified graphene.

Acknowledgements

This work was supported by the Program for New Century Excellent Talents in University (NCET-10-0035), National Natural Science Foundation of China (Grant no. 51373005, 21204087), National Key Basic Research Program of China (2014CB931800) and Fundamental Research Funds for the Central Universities.

Notes and references

1 K. S. Novoselov, A. K. Geim, S. Morozov, D. Jiang, Y. Zhang, S. Dubonos, I. Grigorieva and A. Firsov, *Science*, 2004, **306**, 666.
2 Y. Zhang, Y.-W. Tan, H. L. Stormer and P. Kim, *Nature*, 2005, **438**, 201.
3 F. Schedin, A. Geim, S. Morozov, E. Hill, P. Blake, M. Katsnelson and K. Novoselov, *Nat. Mater.*, 2007, **6**, 652.
4 Q. Cheng, M. Wu, M. Li, L. Jiang and Z. Tang, *Angew. Chem., Int. Ed.*, 2013, **125**, 3838.
5 X. Li, X. Wang, L. Zhang, S. Lee and H. Dai, *Science*, 2008, **319**, 1229.
6 S. Stankovich, D. A. Dikin, G. H. Dommett, K. M. Kohlhaas, E. J. Zimney, E. A. Stach, R. D. Piner, S. T. Nguyen and R. S. Ruoff, *Nature*, 2006, **442**, 282.
7 S. Watcharotone, D. A. Dikin, S. Stankovich, R. Piner, I. Jung, G. H. Dommett, G. Evmenenko, S.-E. Wu, S.-F. Chen and C.-P. Liu, *Nano Lett.*, 2007, **7**, 1888.
8 T. Ramanathan, A. Abdala, S. Stankovich, D. Dikin, M. Herrera-Alonso, R. Piner, D. Adamson, H. Schniepp, X. Chen and R. Ruoff, *Nat. Nanotechnol.*, 2008, **3**, 327.

9 X. Du, I. Skachko, A. Barker and E. Y. Andrei, *Nat. Nanotechnol.*, 2008, **3**, 491.
10 D. Chen, H. Feng and J. Li, *Chem. Rev.*, 2012, **112**, 6027.
11 F. Yavari and N. Koratkar, *J. Phys. Chem. Lett.*, 2012, **3**, 1746.
12 Y. JuáYun, H. JuáPark, S. EonáMoon and B. HoonáKim, *Nanoscale*, 2014, **6**, 6511.
13 Y. Yang, C. Tian, J. Wang, L. Sun, K. Shi, W. Zhou and H. Fu, *Nanoscale*, 2014, **6**, 7369.
14 Q. He, S. Wu, Z. Yin and H. Zhang, *Chem. Sci.*, 2012, **3**, 1764.
15 A. Lipatov, A. Varezhnikov, P. Wilson, V. Sysoev, A. Kolmakov and A. Sinitskii, *Nanoscale*, 2013, **5**, 5426.
16 D. Li, M. B. Müller, S. Gilje, R. B. Kaner and G. G. Wallace, *Nat. Nanotechnol.*, 2008, **3**, 101.
17 Y. Hernandez, V. Nicolosi, M. Lotya, F. M. Blighe, Z. Sun, S. De, I. McGovern, B. Holland, M. Byrne and Y. K. Gun'Ko, *Nat. Nanotechnol.*, 2008, **3**, 563.
18 I. Jung, D. A. Dikin, R. D. Piner and R. S. Ruoff, *Nano Lett.*, 2008, **8**, 4283.
19 W. Yuan, A. Liu, L. Huang, C. Li and G. Shi, *Adv. Mater.*, 2013, **25**, 766.
20 S. Srinivasan, S. H. Je, S. Back, G. Barin, O. Buyukcakir, R. Guliyev, Y. Jung and A. Coskun, *Adv. Mater.*, 2014, **26**, 2725.
21 H.-W. Yu, H. K. Kim, T. Kim, K. M. Bae, S. M. Seo, J.-M. Kim, T. J. Kang and Y. H. Kim, *ACS Appl. Mater. Interfaces*, 2014, **6**, 8320.
22 H. Zhang, J. Feng, T. Fei, S. Liu and T. Zhang, *Sens. Actuators, B*, 2014, **190**, 472.
23 W. Li, Y. Kim and M. Lee, *Nanoscale*, 2013, **5**, 7711.
24 T. Aida, E. Meijer and S. Stupp, *Science*, 2012, **335**, 813.
25 E. Busseron, Y. Ruff, E. Moulin and N. Giuseppone, *Nanoscale*, 2013, **5**, 7098.
26 Q. Zhou, Y. Li, Q. Li, Y. Wang, Y. Yang, Y. Fang and C. Wang, *Nanoscale*, 2014, **6**, 8387.
27 S. Liu, B. Yu, H. Zhang, T. Fei and T. Zhang, *Sens. Actuators, B*, 2014, **202**, 272.
28 L. Huang, Z. Wang, J. Zhang, J. Pu, Y. Lin, S. Xu, L. Shen, Q. Chen and W. Shi, *ACS Appl. Mater. Interfaces*, 2014, **6**, 7426.
29 Y. H. Su, Y. K. Wu, S. L. Tu and S.-J. Chang, *Appl. Phys. Lett.*, 2011, **99**, 163102.
30 W. Zhang, F. Li, Y. Hu, S. Gan, D. Han, Q. Zhang and L. Niu, *J. Mater. Chem. B*, 2014, **2**, 3142.
31 Q. Su, S. Pang, V. Alijani, C. Li, X. Feng and K. Müllen, *Adv. Mater.*, 2009, **21**, 3191.
32 Y. Q. Li, T. Yu, T. Y. Yang, L. X. Zheng and K. Liao, *Adv. Mater.*, 2012, **24**, 3426.
33 W. Shao, X. Liu, H. Min, G. Dong, Q. Feng and S. Zuo, *ACS Appl. Mater. Interfaces*, 2015, **7**, 6966.
34 P. Bazant, I. Kuritka, L. Munster and L. Kalina, *Cellulose*, 2015, **22**, 1275.
35 M. E. Franke, T. J. Koplin and U. Simon, *Small*, 2006, **2**, 36.
36 N. Barsan, D. Koziej and U. Weimar, *Sens. Actuators, B*, 2007, **121**, 18.
37 J. Che, L. Shen and Y. Xiao, *J. Mater. Chem.*, 2010, **20**, 1722.
38 Y. Si and E. T. Samulski, *Nano Lett.*, 2008, **8**, 1679.

